
Effects of fracture lineaments and in-situ rock stresses on groundwater flow in hard rocks: a case study from Sunnfjord, western Norway

Helge Henriksen · Alvar Braathen

Abstract Systematic field mapping of fracture lineaments observed on aerial photographs shows that almost all of these structures are positively correlated with zones of high macroscopic and mesoscopic fracture frequencies compared with the surroundings. The lineaments are subdivided into zones with different characteristics: (1) a central zone with fault rocks, high fracture frequency and connectivity but commonly with mineral sealed fractures, and (2) a damage zone divided into a proximal zone with a high fracture frequency of lineament parallel, non-mineralized and interconnected fractures, grading into a distal zone with lower fracture frequencies and which is transitional to the surrounding areas with general background fracturing. To examine the possible relations between lineament architecture and in-situ rock stress on groundwater flow, the geological fieldwork was followed up by in-situ stress measurements and test boreholes at selected sites. Geophysical well logging added valuable information about fracture distribution and fracture flow at depths. Based on the studies of in-situ stresses as well as the lineaments and associated fracture systems presented above, two working hypotheses for groundwater flow were formulated: (i) In areas with a general background fracturing and in the distal zone of lineaments, groundwater flow will mainly occur along fractures parallel with the largest in-situ rock

stress, unless fractures are critically loaded or reactivated as shear fractures at angles around 30° to σ_H ; (ii) In the influence area of lineaments, the largest potential for groundwater abstraction is in the proximal zone, where there is a high fracture frequency and connectivity with negligible fracture fillings. The testing of the two hypotheses does not give a clear and unequivocal answer in support of the two assumptions about groundwater flow in the study area. But most of the observed data are in agreement with the predictions from the models, and can be explained by the action of the present stress field on pre-existing fractures.

Résumé La cartographie systématique des linéaments de fracture observés sur les photos aériennes montrent que ces structures sont positivement corrélés avec des zones macroscopiques et mésoscopiques de fréquences notables de fracture en comparaison avec leur entourage. Les linéaments sont subdivisés en zones de différentes caractéristiques : (1) une zone centrale de roches faillées, une fréquence de fracturation importante et une certaine connectivité mais fréquemment des fractures minéralement comblés (2) une zone d'accident divisée en une zone proche avec une fréquence intense de linéaments parallèles, non minéralisés et ne se recoupant pas, évoluant vers une zone de transition avec de faibles fréquences de fracturation et plus loin une zone avec un fond général de fracturation. Pour examiner la possible corrélation entre l'architecture des linéaments et le degré de stress de l'écoulement des eaux souterraines, les levés géologiques de terrain ont été complétés par des essais de stress sur les écoulements des eaux souterraines et des essais de puits sur des sites sélectionnés. Les sondages géophysiques ajoutent une information valorisante sur la distribution des fractures et l'écoulement de fracture en profondeur. Basés sur l'étude du stress in-situ ainsi que sur les linéaments et les systèmes associés de fractures présentés précédemment, deux hypothèses de travail ont été développées : (i) Dans les zones présentant un simple fond de fracturation et dans les zones de transition des linéaments, l'écoulement des eaux souterraines est localisé dans les linéaments parallèles avec le stress in-situ le plus important, à moins que les fractures soient chargées ou réactivées comme des fractures de cisaillement avec des angles entre 30 et 0° , (ii) dans la zone d'influence des linéaments, le meilleur potentiel

Received: 31 March 2004 / Accepted: 18 January 2005
Published online: 9 April 2005

© Springer-Verlag 2005

H. Henriksen (✉)
Sogn og Fjordane University College, Faculty of Engineering
and Science,
P.O. Box 133,
N-6851 Sogndal, Norway
e-mail: helge.henriksen@hisf.no
Tel.: +47-57676232
Fax: +47-57676201

H. Henriksen
Department of Earth Science, University of Bergen,
Allégaten 41,
N-5007 Bergen, Norway

A. Braathen
Centre for Integrated Petroleum Research,
Realfagbygget Allégaten 41,
N-5007 Bergen, Norway
e-mail: alvar.braathen@cipr.uib.no

pour l'exploitation des eaux souterraines est dans la zone proche, où la fréquence de fracturation est très importante, de même que la connectivité, avec des remplissages de fracture négligeables. L'essai de validation de ces deux hypothèses ne donne pas une réponse claire et univoque sur les deux hypothèses de l'eau souterraine dans la zone d'étude. Néanmoins la plus part des données observées sont en accord avec la prédiction des modèles, et peuvent être expliquées par l'action de contraintes du sol sur les fractures pré-existantes.

Resumen El mapeo sistemático de campo de lineamientos-fractura observados en fotografías aéreas muestra que casi todas estas estructuras se correlacionan positivamente con zonas macroscópicas y mesoscópicas de alta frecuencia de fracturamiento en comparación con los alrededores. Los lineamientos se subdividen en zonas con características distintas: (1) una zona central con rocas de falla, fracturamiento de alta frecuencia y conectividad pero frecuentemente con fracturas selladas con minerales, y (2) una zona dañada dividida en una zona próxima con fracturamiento de alta frecuencia de lineamientos paralelos, no mineralizada, y fracturas interconectadas graduando a una zona alejada con frecuencia de fracturamiento menor y la cual es transicional a las áreas vecinas con fracturamiento de fondo general. Para examinar las relaciones posibles entre la estructura de los lineamientos y los esfuerzos de la roca in-situ en el flujo de agua subterránea se continuó el trabajo geológico de campo con mediciones in-situ de esfuerzos y pruebas en pozos en sitios seleccionados. El registro geofísico de pozos agregó información valiosa acerca de la distribución de fracturas y el flujo en fracturas a profundidad. Basado en los estudios de esfuerzos in-situ así como también en los lineamientos y sistemas de fractura asociados que se presentaron arriba se han formulado dos hipótesis de trabajo para el flujo de agua subterránea: (i) en áreas con fracturamiento de fondo general y en la zona lejana de lineamientos, el flujo de agua subterránea ocurrirá principalmente a lo largo de fracturas paralelas con los esfuerzos más grandes in-situ de la roca, a menos que las fracturas estén críticamente cargadas o reactivadas como fracturas de cizalla en ángulos que varían de 30° a 0°, (ii) en el área de influencia de lineamientos, el mayor potencial para la abstracción de agua subterránea se encuentra en la zona próxima, donde existe una frecuencia de fracturamiento alta y conectividad con relleno de fracturas insignificante. La evaluación de las dos hipótesis no aporta una respuesta clara e inequívoca en apoyo de los dos supuestos acerca del flujo de agua subterránea en el área de estudio. Sin embargo, la mayoría de datos observados concuerda con las predicciones de los modelos lo cual puede explicarse por la acción del campo de esfuerzos actual sobre las fracturas preexistentes.

Keywords Fractured rocks · Geophysical methods · Groundwater flow · Tectonics · Conceptual models

Introduction

The crystalline metamorphic rocks in Norway mostly lack any primary porosity and permeability, and practically all storage and transport of groundwater is related to the secondary fracture network in the rock mass. Due to their heterogeneity, well yield in crystalline hard rocks possessing only secondary porosity and permeability is difficult to predict and displays a wide variation. It may differ from one rock type to another, and even for a given rock type, the yields of adjacent wells may differ by many orders of magnitude.

These differences are caused by a combination of both independent and interrelated factors that may influence the hydrological and geological characteristics of the well sites. Some of these factors are important at the local scale, others at the sub-regional scale, and still others at the regional scale. Regional-scale factors include net precipitation, runoff, and regional stresses, which can produce gradual changes in rock permeability (Rohr-Torp 1994; Gudmundsson 1999; Krásný 2002; Henriksen 2003). More local factors include topography, rock type, overburden, structural position, joint and fracture characteristics, and recharge from surface water bodies (Brook 1988; Henriksen 1995; Mabee 1998; Morland 1997). Henriksen (2003) describes the relative importance of regional and local factors on well yield, the latter being strongly dependent on hydraulic properties such as permeability and hydraulic conductivity of the rock mass. This evaluation was based on the Fennoscandian region of Norway and Sweden, a land area of about 323,000 km².

In this work, focus is set on a much smaller scale where regional factors were considered constant. The area under consideration is the Sunnfjord area (ca. 3,300 km²), about 1% the size of the Fennoscandian region of Norway and Sweden (Fig. 1). This paper summarizes the main results of a project carried out in 1997–2000 led by the Norwegian Geological Survey (NGU) in collaboration with scientific staff and students from the University of Bergen (UiB), Sogn og Fjordane University College (HSF) and the Norwegian University of Science and Technology (NTNU). The focus of the project was first set on systematic field mapping of lineaments observed on satellite photographs. Almost all of the lineaments are bedrock structures that correlate with zones of high macroscopic and mesoscopic fracture frequencies compared with the surroundings, and could thus act as preferred conduits for groundwater flow. The fracture lineaments are subdivided into zones with different characteristics: (1) a central zone with fault rocks, high fracture frequency and connectivity but commonly with mineral sealed fractures, and (2) a damage zone subdivided into a proximal zone with a high fracture frequency of lineament parallel, non-mineralized and interconnected fractures, grading into a distal zone with larger variation in fracture orientation and lower fracture frequencies. This zone is transitional to the surrounding areas with general background fracturing.

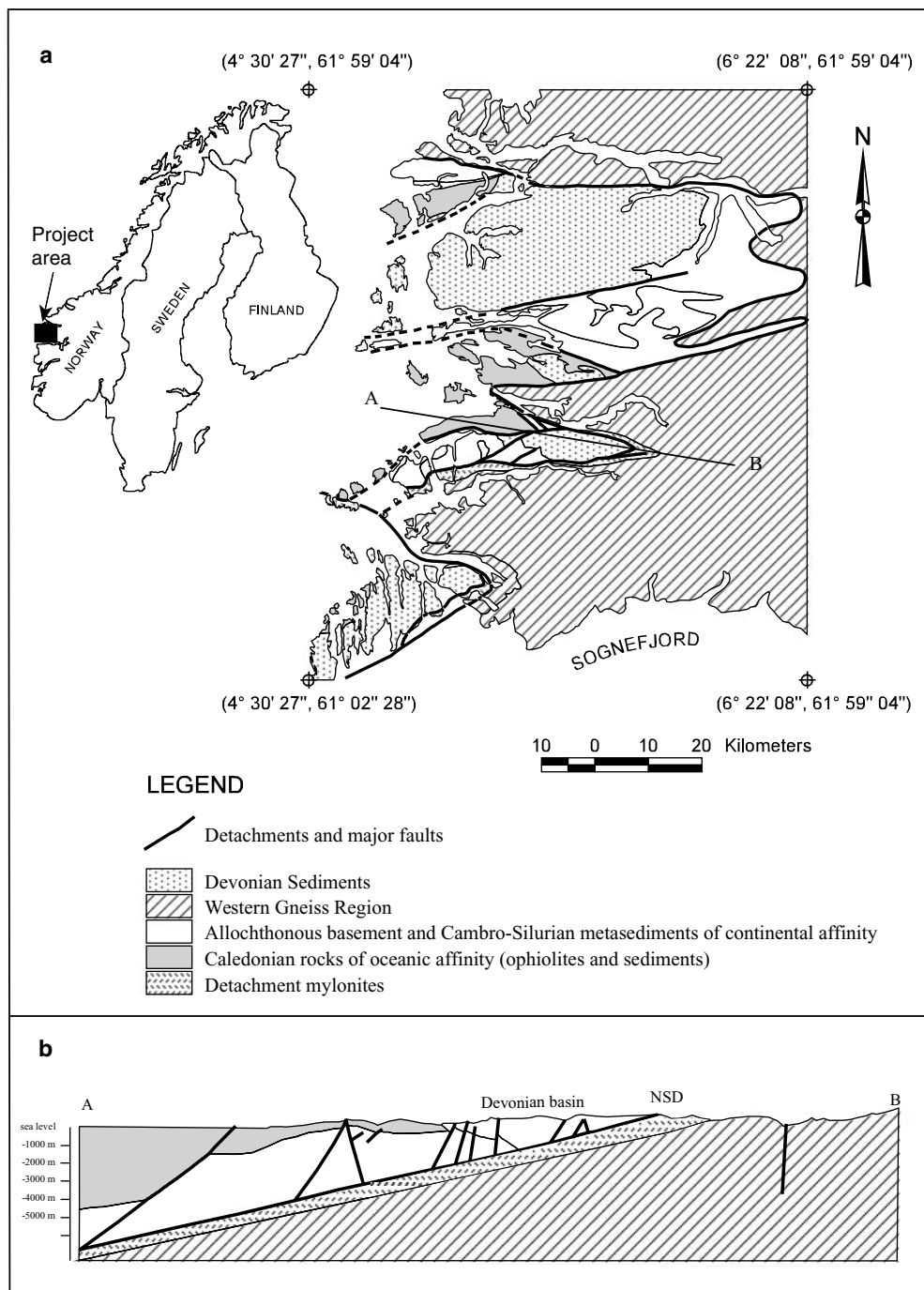


Fig. 1 **a** Simplified geological map of the Sunnfjord area. Modified from Osmundsen and Andersen (1994); **b** Simplified E–W cross section from A to B in Fig. 1a, modified from Braathen et al. (2004). Same legend as in Fig. 1a. *NSD* Nordfjord-Sogn Detachment

Measured in-situ stresses are compressive and are probably the result of a combination of ridge push, postglacial crustal uplift during the Late Holocene and gravity-induced stresses. They are normally in the range of 10–20 MPa, but may exceed 30 MPa (Fejerskov et al. 2000; Midtbø 1996). It is suspected that such high in-situ stresses may also affect the rock mass permeability.

To examine the possible relations between lineament architecture and in-situ rock stress on groundwater flow, the geological fieldwork was followed up by geophys-

ical ground surveys (Elvebakk and Lauritsen 1997), the establishment of test boreholes, and in-situ stress measurements at selected sites (Braathen et al. 1998; Braathen et al. 1999). In addition, geophysical follow up work with well logging and optical televiewer methods (Elvebakk et al. 2002; Elvebakk and Rønning 2002) have added valuable information about fracture distribution and fracture flow at depths.

Based on the studies of the lineaments and associated fracture systems and the in-situ rock stresses, two working

hypotheses for groundwater flow in this region were formulated:

1. In areas with a general background fracturing and in the distal zone of lineaments, the in-situ stress field exerts a major influence on groundwater fracture flow (Braathen et al. 1998), unless fractures in the rock mass are reactivated as shear fractures.
2. In the influence area of lineaments, the largest potential for groundwater abstraction is in the proximal zone, where there is a high fracture frequency and connectivity and commonly negligible fracture fillings (Braathen et al. 1999).

Hypothesis (i) was tested at a well site with nine wells in Holmedal, while hypothesis (ii) was tested at four locations where test boreholes were drilled across selected lineaments at Vadheim, Tysse, Folvåg and Herstad (Fig. 2).

Regional geologic setting

The Sunnfjord area forms a part of the western Norwegian Caledonides. Within this area, Precambrian gneisses of the Western Gneiss Region (WGR) are structurally overlain by Caledonian thrust sheets and low-grade metasediments of Middle Devonian age (Fig. 1a, b).

The gneisses of the Western Gneiss Region are essentially heterogeneous orthogneisses of broadly granitic composition with minor inclusions of basic and ultrabasic rocks and paragneisses. The Caledonian thrust sheets comprise Cambrian–Ordovician units of oceanic affinity (greenstones, greenschists and metagabbro with overlying sediments) as well as tectonic units of Precambrian high-grade basement with low-grade sedimentary cover rocks. In the later years, detailed structural studies have thrown considerable light upon the Early Paleozoic tectonic history of these rocks (Andersen and Jamtveit 1990; Osmundsen and Andersen 1994; Andersen 1998). Following penetrative contractional deformation and southeasterly directed thrusting during continental collision in the Middle Silurian, the thickened orogenic wedge of Precambrian and Lower Paleozoic rocks became unstable and was subjected to westerly directed backsliding along a major westerly dipping low-angle normal fault, termed the Nordfjord-Sogn Detachment (NSD) by Norton (1987). The footwall of the NSD is occupied by the Precambrian gneisses of the Western Gneiss Region. Within the hanging wall, the Caledonian allochthonous units are unconformably overlain by Devonian coarse clastic sediments, which are related to tectonically controlled sedimentation in the Lower to Middle Devonian during the extension of the orogen (Osmundsen and Andersen 2001). Movements along the NSD are believed to mirror the exhumation of the region, with a history that extends through the seismogenic crust and into the aseismic lower crust. This is illustrated by the presence of a varied succession of ductile and brittle fault rocks, depending on their crustal depths during extension and unroofing of the fault zone (Braathen et al. 2004). The main fault displacement took place during the Devonian

and possibly Early Carboniferous (Eide et al. 1999; Braathen et al. 2004), but renewed activity in the Permian and the Late Jurassic–Early Cretaceous is documented (Eide et al. 1997).

Fracturing, faults and tectonics

The hydraulic properties of crystalline rocks are largely dependent on the mechanical and geometrical properties of the fracture network within the rock mass (e.g. NRC 1996). The fracture network in an area is generally the result of repeated brittle deformational episodes, each imposing upon the rock mass faults and fractures of different orientations and physical characteristics (Braathen 1999). The hard rock environment in the vicinity of large fault zones are commonly associated with areas of enhanced fluid flow compared with the surroundings (Barton et al. 1995; Caine et al. 1996). However, fault zone permeability may vary across the fault zones, both in space and time (Evans et al. 1997). Moreover, the water conducting capacity of a particular fault or fracture varies with its orientation in the in-situ stress field. Hence, since the fractures found at a particular well site most likely belong to larger regional fracture systems, an understanding of the regional fracture pattern and the stress regimes under which the fractures developed, as well as the magnitude and orientation of the current crustal stresses, is a necessity in order to elucidate the subsurface water flows inferred during the borehole studies.

Timing and significance of brittle fracturing events

Following the penetrative ductile deformation during the Caledonian orogeny, a series of brittle deformational events in Permian–Jurassic times have affected the off- and on-shore areas of western Norway (Eide et al. 1997; Braathen 1999; Valle et al. 2002; Braathen et al. 2004), producing a complex network of faults, fractures and lineaments. Based on detailed structural studies in the Sunnfjord area (Braathen and Henriksen 1997; Braathen 1999) the following sequence of brittle faulting and shear-fracturing post-dating the major Devonian extensional deformation is recognized and summarized in Table 1.

In addition, it is suspected that the older fractures have suffered neotectonic reactivation. A model by Gudmundsson has shown that the contemporary compressive stress field associated with the ongoing postglacial uplift of Fennoscandia, which started ca. 10,000 years ago, alone could be capable of reactivating existing faults in this area.

Lineament analysis

The regional fracture pattern was assessed by tracing of lineaments from 1: 100,000 scale black-and-white prints

Table 1 Sequence of post Late Devonian fault evolution in the Sunnfjord area based on Braathen and Henriksen (1997) and Braathen (1999)

Fracture population	Type of structure(s)	Dynamic Interpretation	Age of event
1	E–W brittle thrusts and associated reverse faults	N–S (NW–SE) contraction by thrusting and folding	Late Devonian or Early Carboniferous
2	Conjugate NE–SW and NW–SE strike slip faults with bisecting N–S normal faults	N–S shortening and E–W extension related to regional E–W folding	Late Devonian or Early Carboniferous
3	Low-angle NNE–SSW normal faults with fault breccias	ESE–WNW extension	Late Permian
4	Steep E–W striking normal faults	N–S extension	Late Jurassic–Early Cretaceous
5	Reactivation of some of the earlier brittle structures	Neotectonic reactivation	Holocene

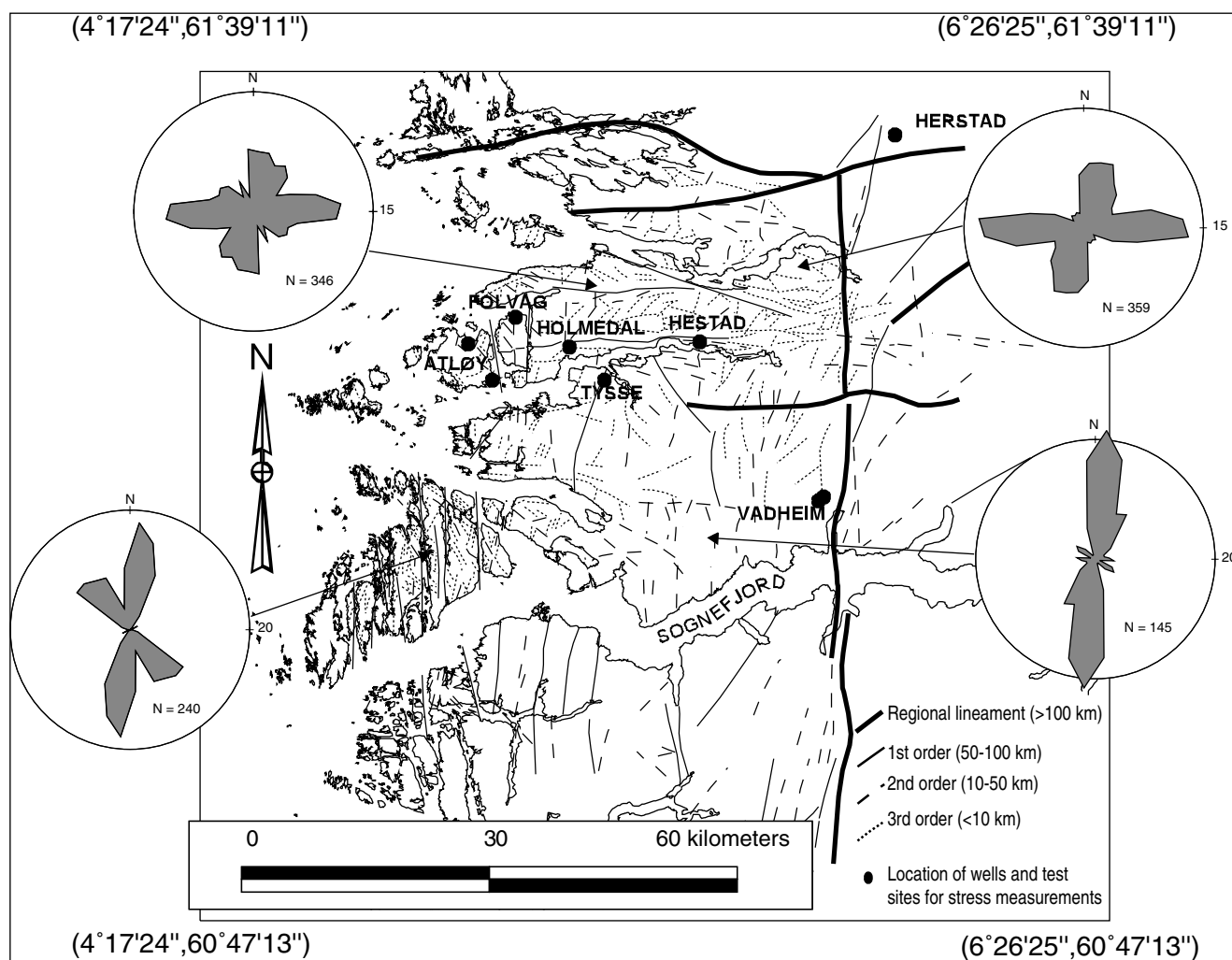


Fig. 2 Lineament map traced from 1: 100,000 Landsat TM scene, band 5. Each *rose diagram* summarizes the orientation of lineaments in the respective quadrangles of the lineament map, and the scale is

frequency in percent of counted lineaments. Locations of test sites are also shown

(spectral band 5) Landsat satellite photographs. This was followed by inspection of the mapped photo-lineaments in the field, confirming that the lineaments almost uniquely coincide with structural bedrock features related to increased frequencies of joints, shear fractures and smaller faults, and layers and lenses of fault rocks. Hence, the lin-

eaments classify as faults. The lineaments in this largely barren region are also clearly manifested as strong physiographic features on 1: 50,000 and 1: 5000 scale topographic maps. In the field studies, orientation of the lineament associated fractures and kinematic indicators on fracture surfaces were also measured. Subtly expressed lineaments,

representing foliations and lithological contacts, were excluded from the final lineament map (Fig. 2). Lineament statistics were derived from a standardized lineament map in a GIS environment applying the method outlined by Kim et al. (2004).

The most prominent lineaments have N–S and E–W orientations. They are present at all scales, from regional lineaments longer than 100 km to 3rd order lineaments with lengths between 1 and 10 km (Fig. 2). In addition, subordinate NE–SW and NW–SE populations of 2nd and 3rd order lineaments with lengths less than 50 km are ubiquitously present. The lineament analysis, supported by field checking, confirms that most N–S lineaments do not significantly displace lithological markers and appear as zones of intense fracturing with breccias in the central parts. Fractures and mesoscopic faults associated with the N–S lineaments can be grouped in two systems: (1) NNW–SSE-oriented tensional fractures and minor sinistral shear fractures at small angles to the lineament direction, and (2) N–S steeply dipping normal faults with associated sets of conjugate NE–SW and NW–SE strike/oblique-slip faults (Braathen et al. 1999; Braathen 1999). The meso-structures are compatible with a development of the N–S lineaments initially as semi-ductile shear zones of en-echelon joints subsequently modified by continued sinistral shear in a NNW–SSE contractional regime. Later reactivation by dextral shear in a N–S contractional regime is suggested by the truncation of the earlier structures by dextral shear fractures. Hence, the N–S lineaments can be explained as immature faults and/or deep, regional, tensile fractures, which have accommodated repeated episodes of reactivation. The N–S lineaments thus have a complex history, and also appear to have been reactivated as group 2 normal faults (see Table 1).

Contrary to the N–S structures, E–W lineaments can be demonstrated to be major faults which significantly displace lithological markers and also truncate the N–S lineaments. Typically, these major E–W faults are found as southern and northern boundary faults of the Devonian basins, extending into the basement gneisses in the east (Fig. 1). Fault movements are multiple, and both Permian and Jurassic–Cretaceous movements have been documented (Eide et al. 1997). At many sites, the E–W lineaments contain non-cohesive fault rocks, which may be signs of recent activity (Braathen et al. 2004).

Both the N–S and E–W lineaments were recognized by Gabrielsen et al. (2002) as prominent regional lineaments in Norway that reflect repeated tectonic activity since the Neoproterozoic (600–550 Myr ago). NW–SE and NE–SW lineaments are widely recognized throughout the Baltic Shield area, and probably represent an old megafault pattern that may date as far back as the Archaean (Ramberg et al. 1977; Gabrielsen et al. 2002).

Lineament architecture and fracture distribution

In order to obtain information about the fracture distribution in and near lineaments, fractures were mapped along profiles running perpendicular to N–S and E–W-oriented lin-

eaments in lithologies as diverse as Precambrian basement gneisses, Caledonian metasediments and metavolcanics, and Devonian, very low-grade metasediments. Both the azimuth vs. traverse distance method (Wise and McCrory 1982) and traverse methods (Goldstein and Marshak 1988) were used. In the azimuth vs. traverse distance method, each fracture profile consisted of station sites 5 m apart, where all fractures crossing a sampling circle with diameter 80 cm were measured and counted. The fracture frequency at each station was defined as the number of through-going fractures crossing the perimeter of the sampling circle at two points. Hence the minimum length of any measured fracture is about 20 cm, and most of the measured fractures are longer than 70–80 cm. Strike and dip of fractures were measured and sense of movement indicators were recorded where present. Profile lengths were typically ca. 2–300 m, but longer traverses (up to 6 km) were also measured in order to assess the background frequency. With this method, fracture data were collected along 40 profiles, 22 on N–S lineaments and 18 on E–W lineaments.

Figure 3 shows a frequency vs. distance plot of fracture data collected by the azimuth vs. traverse distance method from a 6 km long traverse crossing two prominent 2nd order N–S lineaments in the Holmedal area. In Fig. 3b, fracture frequencies are calculated as a moving median of ten adjacent measuring stations. The plot depicts a background level with fracture frequencies of 0–2 above which are isolated highs with frequencies larger than 3. The highs coincide with inclusions of competent rocks such as granitic gneisses and meta-gabbros in the otherwise micaceous and phyllonitic rocks along the profile, but close to the major lineaments enhanced fracture frequencies are encountered regardless of rock type.

Individual profile plots for the traverses across the 22 N–S and the 18 E–W lineaments display some variation in fracture frequencies and distribution. But when the fracture frequency data for the N–S and the E–W lineaments are aggregated into single data sets, and fracture frequency is plotted against distance to lineament centre, a strong positive correlation between proximity to lineament and fracture frequency is demonstrated (Braathen and Gabrielsen 1998). However, while the N–S lineaments show symmetrical fracture frequency patterns, the E–W faults show an asymmetric pattern with more intense fracturing in the hanging wall.

With the traverse inventory method, all fractures intersecting a pre-selected traverse line within one meter intervals were counted and measured. This method was applied to the collection of detailed fracture data such as fracture spacing and length, aperture, connectivity, fracture mineralization and kinematic indicators from 35 profiles varying in length from less than one meter to 40 m (Braathen et al. 1999).

In conclusion, an area within ca. 250–300 m of any large lineament is affected by enhanced fracturing, and the fracture orientations and frequencies vary as a function of the distance from the lineaments (Braathen and Gabrielsen 1998). Lineament-parallel fractures predominate close to the lineaments, whereas oblique fractures

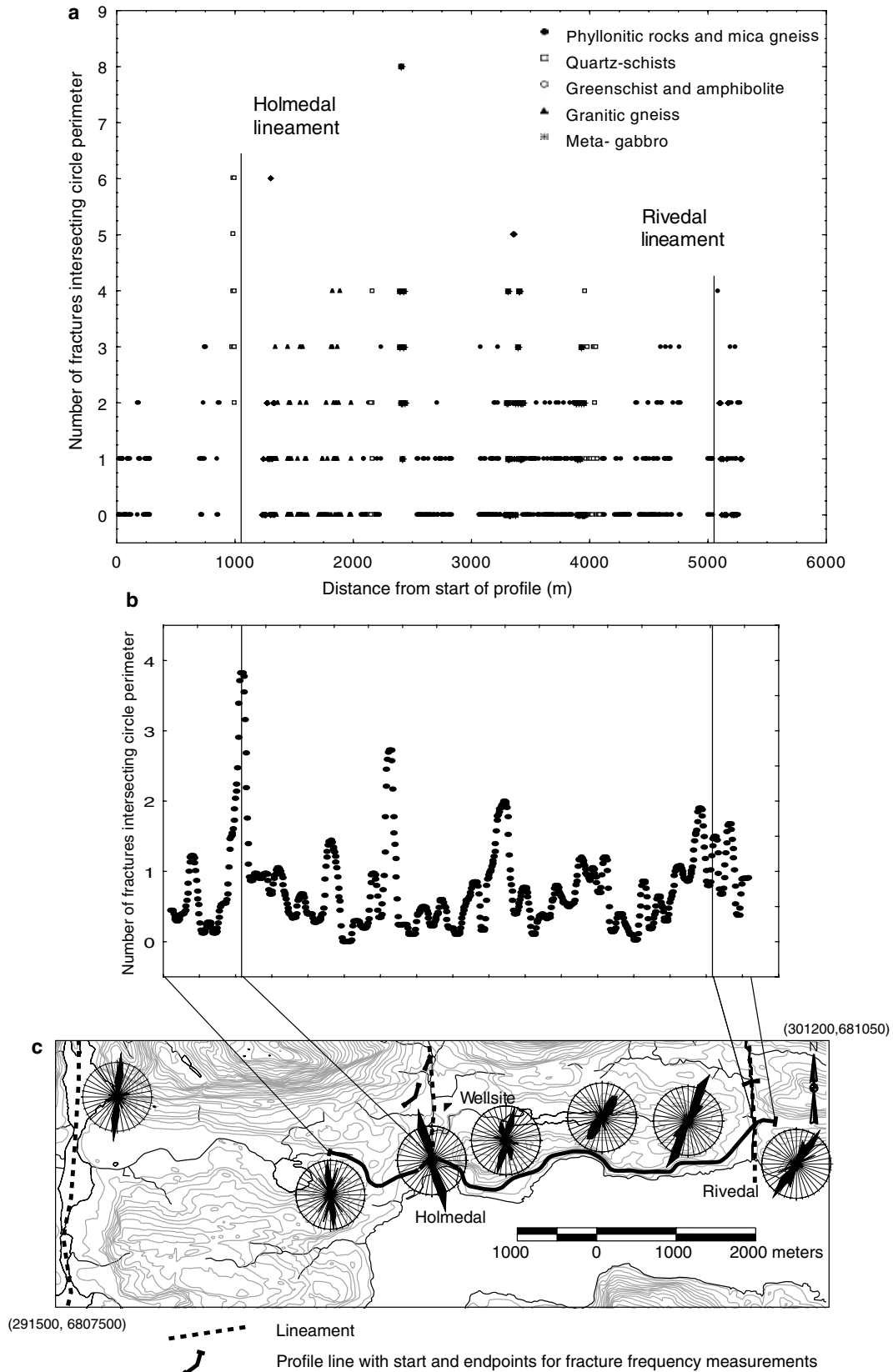


Fig. 3 Fracture frequency diagram for E-W profile with starting point west of Holmedal. The measurements are from vertical road-sections, and the distances are the projected distances perpendicular to the two parallel fracture zones; **a** Frequencies vs. distance; **b** Run-

ning median plot of frequencies vs. distance; **c** Location of profile lines with *rose diagrams* of fracture orientations along the profile. The Holmedal well site is also shown

dominate at greater distances. Based on criteria such as distribution and orientation of fractures, as well as type of fault rocks, mineralization and fracture geometries, the 250–300 m wide deformation zone about the lineaments may be subdivided into: (1) a central part (0–20 m width) of high fracture frequency with a network of short fractures subparallel to the lineament trend and local fault rocks, (2) a proximal part (10–50 m width) of high fracture frequency with dominantly lineament subparallel fractures, fringed by a system of intersecting oblique fractures and (3) a distal part (up to 200 m width) of low fracture frequency where oblique fractures dominate. At a distance of 250–300 m from the lineament, a background fracture system with fracture orientations clearly different from the lineament-related fractures is encountered. The topographic expression of the lineaments in general coincides with the margin of the proximal part.

This subdivision of the lineament is an idealized model, and the deformation zones described above may be variably developed in terms of fault rock types and fracturing characteristics from lineament to lineament, depending on such factors as lithology, strain intensity and strain-rate, deformational history and degree of reactivation. Especially the central part of a lineament may be thin or absent in lineaments with a simple deformation history. As mentioned, vertical and subvertical fracture lineaments tend to have a symmetrical distribution of their deformation zones, whereas inclined faults have accommodated most of the strains in their hanging walls.

Fracture enhanced permeability depends on density of fractures, fracture length and aperture and connectivity (Singhal and Gupta 1999). Although the central part of the lineaments studied has a high fracture density, it represents a low permeability zone due to the presence of fault rocks such as breccias and occasionally fault gouge, as well as the common presence of secondary mineral fillings in fractures. Shear fractures are the most common fractures. On the contrary, the proximal zone has longer individual fractures of diverse orientations but also with high fracture frequencies, resulting in a fracture network of high connectivity. Although shear fractures are the most abundant, tensional fractures are also common. Secondary mineral fillings in fractures are also in general absent, making the proximal part of the lineament a zone of potential enhanced permeability. Detailed studies of the fracture geometry of the lineaments in Sunnfjord (Braathen et al. 1999; Berg 2000) have shown that fracture aperture and connectivity are about twice as large in the proximity of the fracture lineaments, i.e. in their proximal zone, compared to the distal zone and background areas. Hence, judged by geometry and hydromechanical properties of the contained fractures, the proximal zone should be considered the most permeable structure of the lineaments.

In-situ rock stresses

Within any area, the in-situ regional state of stress controls fracture apertures and the reactivation potential of exist-

ing faults and fractures (Sayers 1990; Banks et al. 1996; Barton et al. 1995), thereby affecting the hydromechanical properties and permeability of the rock mass. If the in-situ stresses are equal to or exceed the mechanical strength of the rock, new fractures may also initiate and propagate through the rock mass. In addition, stress perturbations associated with topography may affect the hydromechanical properties of the rock mass at the local scale (Morin and Savage 2002), and may also be capable of generating new fractures (Chapman 1958; Miller and Dunne 1996; Savage et al. 1985).

The largest horizontal stress (σ_H) has a general E–W to ESE–WNW orientation in the North Sea and outer Sunnfjord area, but a weaker NW–SE trend of σ_H is also present (Lindholm et al. 2000; Fejerskov et al. 2000; Dehls et al. 2000). However, western Norway is characterized by a significant topographic relief, and it is suspected that in-situ measurements are influenced by the local topography (Nilsen and Palstrøm 2000). A compilation of overcoring measurements from 21 tunnels in the central and inner parts of western Norway (Midtbø 1996) shows a NW–SE direction for σ_H in the central and eastern parts of Sogn og Fjordane, but NE–SW directions for σ_H are also present. Both directions are coincident with valley sides, which indicate a considerable influence of gravitative rock stresses.

In connection with the project, in-situ stress measurements by hydraulic splitting technique in shallow (12–23 m) boreholes were carried out at three different locations in outer Sunnfjord (Hansen 1996). The measuring sites on Atløy (Fig. 2) are in regions of low topographic relief, while the locality at Hestad is in an E–W-oriented steep valley side. The orientation of σ_H on Atløy was E–W and NE–SW for the northern and southern sites respectively, and the magnitudes were 7.5 and 6.5 MPa. The site at Hestad (Fig. 2) was chosen to investigate the effects of a steep valley slope on the rock stresses. At this locality, σ_H had an E–W orientation parallel to the valley side and with a magnitude of ca. 15–19.5 MPa and with σ_h of ca. 8–10 MPa, in other words much higher than in the flat terrain of Atløy.

Testing of hypothesis (i): The Holmedal research wellfield

A wellfield was located and configured to test hypothesis (i). Based on the measurements from the nearby sites at Atløy and Hestad, situated ca. 8–10 km from Holmedal, it is considered that σ_H in the research wellfield has an approximate E–W orientation with magnitudes around 7.5–10 MPa, while the least horizontal stress σ_h has a magnitude of ca. 5 MPa.

The research wellfield covers an area of about 1,000 m² and is located in a broad and flat valley bottom (Fig. 4a). Surficial cover is negligible. Although located not more than about 200 m from a 2nd order N–S trending lineament (Fig. 4b) and about 600 m south of an E–W lineament associated with a major population 4 fault (Table 1), the

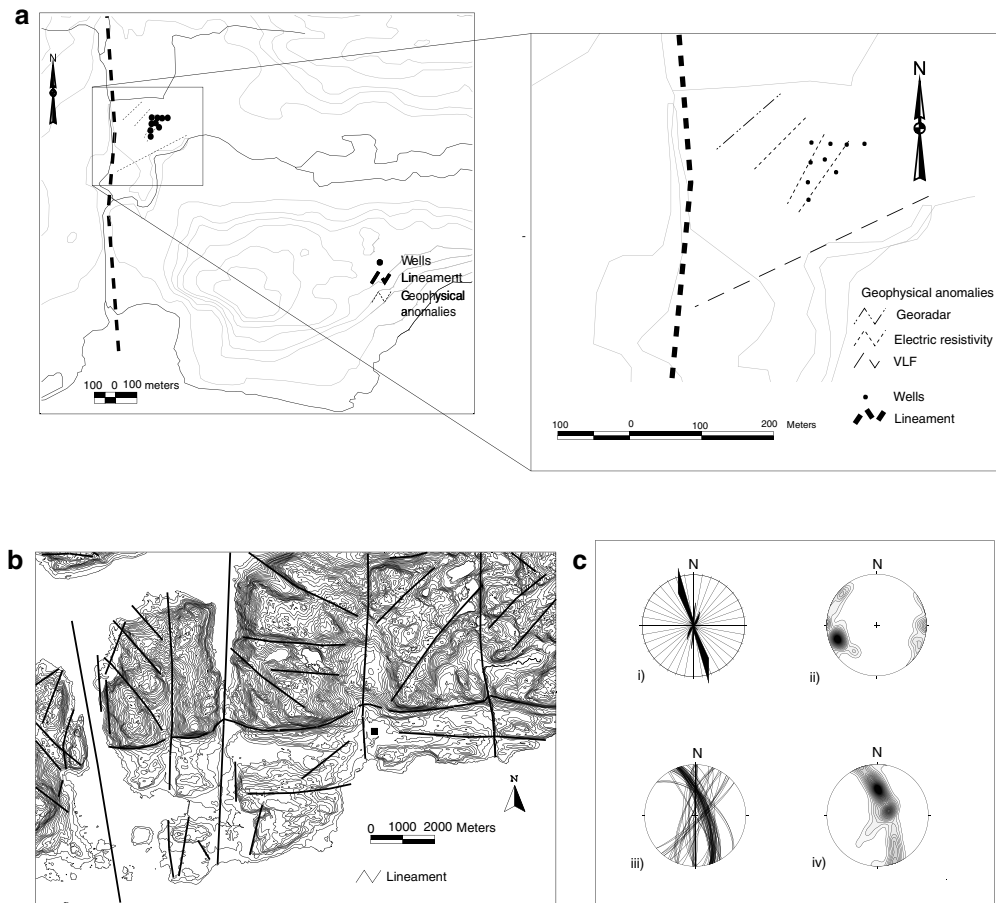


Fig. 4 **a** Overview map of the Holmedal wellfield; **b** Lineament map of the area around Holmedal; **c** Stereographic plots of surface fractures at the wellfield: i) rose diagrams showing azimuth directions of fractures ($N=89$) at the test site; ii) contoured stereographic projection

(lower hemisphere) of the poles to the fracture surfaces; iii) stereographic projection of the fracture surfaces; iv) contoured plot of fracture surface intersections totaling 3914 intersections

influence of lineament associated fracturing is negligible and fracture frequencies are at the background level (Fig. 3). The rocks at the site are dark green amphibolites, which locally develop as chlorite schists in zones of strong deformation. In addition, phyllonitic rocks with suspected igneous precursors are found. The foliation of the rocks dips gently to the north at $20\text{--}50^\circ$. Fracture orientation and frequencies were measured in detail along horizontal scan lines by counting all fractures intersecting 1 m long horizontal sampling lines. All fractures were measured and plotted in rose diagrams and stereographic pole diagrams (Fig. 4c). Most fractures are steep to subvertical with a NNW–SSE or NNE–SSW strike (Braathen et al. 1998). Some E–W striking foliation-parallel fractures, which dips moderately to the north are also present. The two populations of fractures intersect in two main orientations: group 1 which are steeply plunging towards ENE, and group 2 which are plunging in a NNW direction at about 50° (Fig. 4c, iii–iv).

Additional work was conducted by ground geophysical surveys using electrical profiling and ground penetrating radar (Elvebakk and Lauritsen 1997). These results indicate the existence of possible water conducting structures at depth trending ca. $N30^\circ E$, while VLF measurements in-

dicated a fracture zone trending ca. $N70^\circ E$ just south of the wellfield (Fig. 4a).

Pumping tests

The well site (Figs. 4a, 5a) consists of nine vertical, open bedrock wells arranged in a triangular grid. The central well (W9) is 100 m deep, while the other wells were drilled to 50 m depth. Both short-term and long-term pumping tests were performed.

In the short-term pumping tests (Braathen et al. 1998), each of the 9 wells except W7 was pumped while drawdowns in the other wells were continuously recorded. In each test, the water level in the pumping well was lowered to about 50 m and kept at this level for about 1 h before the pumping was stopped. Both drawdowns and the natural rise of the water levels in the wells were continuously monitored with data sampling intervals of 5 s. The total duration of each pumping and recovery test was about 20–24 h. Estimated well capacities based on the pumping tests are summarized in Table 2.

In terms of drawdown and recovery data, there is an immediate and significant two-way hydraulic response between W6, W8 and W9. There are also significant

Table 2 Summary of well data for the Holmedal wellfield

Well no	Depth (m)	Well yield at stable drawdown (l h ⁻¹)	Specific capacity (l h ⁻¹ m ⁻¹)	Well capacity from recovery tests (l h ⁻¹)
W1	50	36	0.8	23
W2	50	55	1.2	54
W3	50	110	2.3	81
W4	50	0	0	6.8
W5	50	15	0.3	3.7
W6	50	54	1.3	132
W7	50	No data	No data	0.8
W8	50	1066	25	860
W9	100	129	3.0	86

one-way hydraulic responses during test pumping between W3 and wells W6, W3 and W8. Small-scale oscillations in water levels, possibly reflecting weak hydraulic responses between wells, are recorded in W1 during pumping of W2, in W1 during pumping of W6, in W2 during pumping from W8, and in W2 and W3 during pumping from W9 (Fig. 5b).

A long-term pumping test of 10 days duration was conducted with W9 as the pumping well (Gaut et al. 1999). The response of the water-level recordings during the pumping test and tracer tests conducted during pumping confirmed the results obtained from the short-term pumping tests of a significant hydraulic connection between W9 and the wells W6, W8 and W3. In addition, possible weak hydraulic

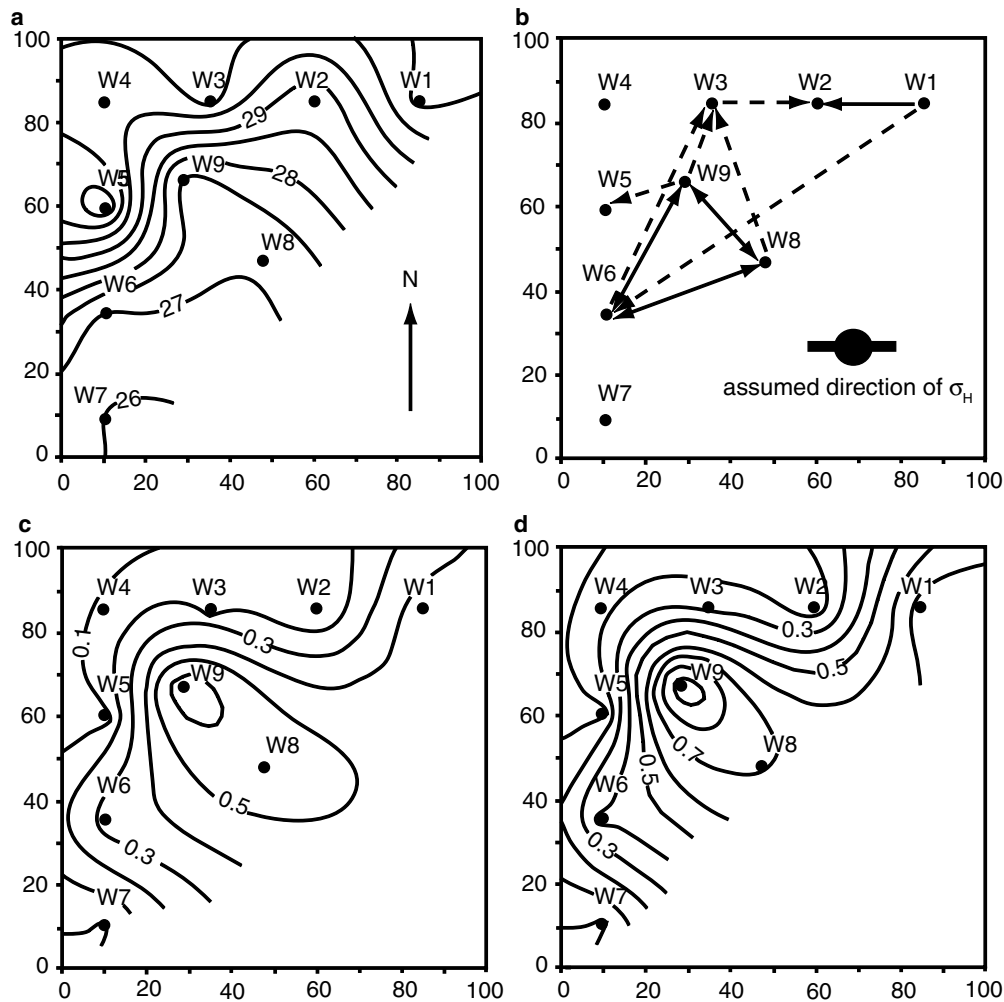


Fig. 5 a Contoured map of natural groundwater levels in W1-W9 prior to test pumping of W9; b Map summarizing the main groundwater flow directions inferred from test pumping; c Contour map of water table drawdowns after 32 h of test pumping; d Contour map of

water table drawdowns after 44 h of test pumping. Figure 7a, c and d are compiled from Gaut et al. (1999), Fig. 7b from Braathen et al. (1998) and Gaut et al. (1999)

connections between W9 and the wells W2 and W5 were indicated (Fig. 5b). W7 stands out as an extreme low capacity well (Table 2) with no hydraulic connection with the other wells.

Geophysical logging

Later borehole geophysical investigations employing natural gamma, fluid temperature and conductivity, resistivity and optical televiever logs were performed in W9 (Elvebakk and Rønning 2002). In addition, acoustic televiever logs were run in wells 1, 2, 3, 4 and 8 (Henning and Elvebakk 2001) and OPTV logs were run in wells (2, 4, 6 and 8). The geophysical logs (Fig. 6a) have provided additional valuable information in characterizing the bedrock aquifer. An important fact is that, contrary to the fracture pattern measured at the surface, the dominating fractures at depth are foliation parallel fractures with E–W strikes and 50–60 degree northerly dips. NNW–SSE fractures are only subordinate (Fig. 6b). Some of the wells, for example W9, show an increase in fracture frequency with depth. In this well, the temperature and conductivity logs indicate water inflows through open E–W fractures at depths of 30.5, 56.5, 88 and 94 m (Fig. 6). The OPTV log for W9 shows very low fracture frequencies down to ca. 50 m depth, but higher frequencies with uniform fracture distributions from 50–100 m. The interval from 54–64 m stands out as a pronounced fracture zone with E–W fracturing. An open E–W fracture depicted by the OPTV log at 60.9–61 m depth correlates with a pronounced low-resistivity zone slightly below 60 m depth (Fig. 6a).

Provided the E–W fracture zone encountered at 54–60 m depth in W9 is a persistent structure, it would also be inter-

sected by W6 and W8, possibly by W5, but not the other wells. A fracture zone indicated by the pumping test of W8 at 11–13 m (Braathen et al. 1998) may possibly be associated with the this fracture zone, as the 50–60° northerly dipping E–W fracture zone intersecting W9 would intersect W8 at approximately this depth interval. Hence, this fracture zone could account for the observed hydraulic responses during the pumping tests.

Relationships of groundwater fracture flow to stress directions

Due to the inherent inhomogeneity of the fractured rock mass, drawdown contour maps are not likely to reveal the true piezometric surface of a bedrock aquifer. However, they may be of great value in evaluation of aquifer anisotropy (Gernand and Heidtman 1997), especially if such plots are produced for different stages during test pumping.

The water table contour map based on measured water levels in the wells prior to test pumping is shown in Fig. 5a. Natural water levels in adjacent wells may differ considerably, and probably reflects that the water level is defined by the piezometric pressure in fracture systems with no hydraulic connection. Water levels in wells W6, W8 and W9 are similar and significantly lower (–3 m) than in the other wells, whose water levels are close to the surface. Judged by the short-term pumping tests and the geophysical data from W9, the hydraulic heads of these three wells are controlled by the single transmissive E–W fracture zone intersecting W9 at 54–64 m depth.

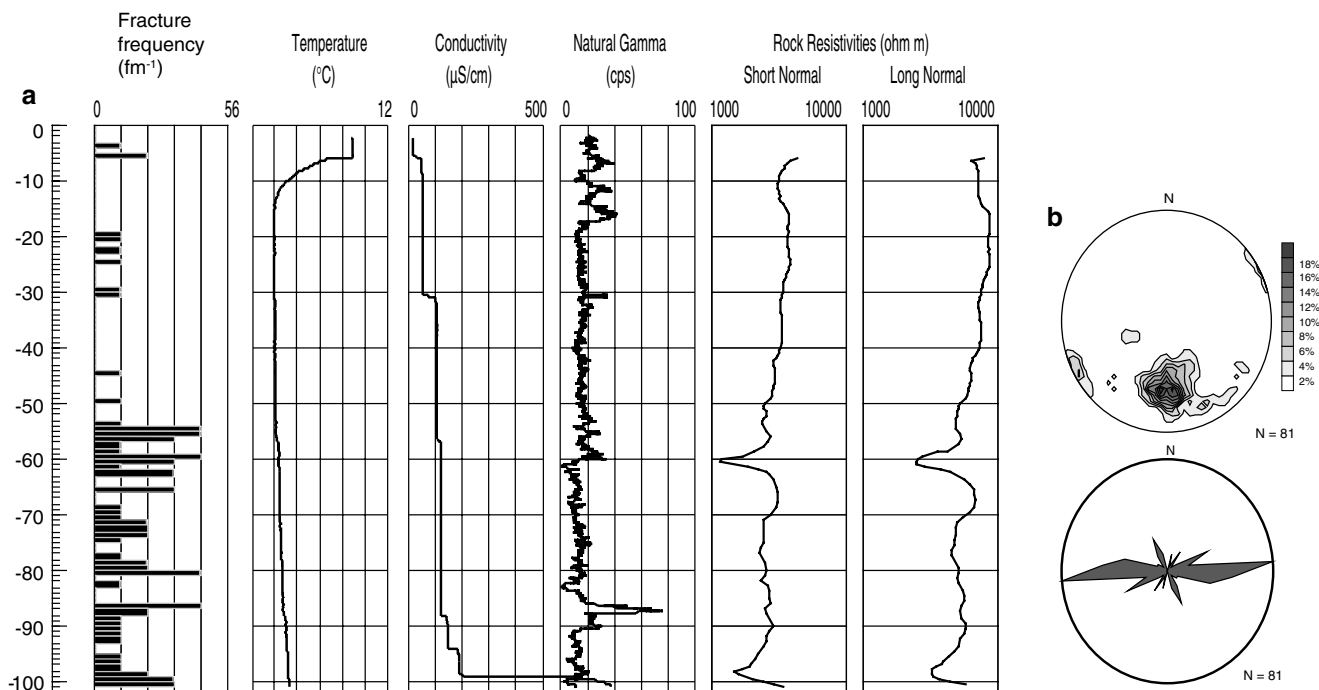


Fig. 6 a Wells logs from W9, Holmedal wellfield, prepared from geophysical data from Elvebakk and Rønning (2002); b Stereographic plot of poles to fractures and *rose diagram* showing orientation of fractures recorded by the OPTV log

The water table contours at the stable situation do not mirror the surface topography and illustrates the anisotropy of the aquifer. The variable hydraulic gradient may be interpreted in terms of groundwater movement towards the area around W7, or in terms of an E–W anisotropy with higher hydraulic conductivities in this direction. The latter explanation is preferred, as W7 appears to be located in a low permeability region with no interconnection with the otherwise fractured aquifer.

The overall picture changes during pumping. The draw-down contour map after 2 days of the long-term pumping test depicts a development of a slightly elongate cone of depression in the water table with an SE–NW directed major axis (Fig. 5c, d), which is consistent with a drawdown related to an SE–NW fracture pattern of higher transmissivity.

Based on the slip and rupture Coulomb–Navier criterion structures oriented at angles $\pm 30^\circ$ to σ_H would be most prone for reactivation by induced shear stresses. Barton et al. (1995) and Ferril et al. (1999) found a positive correlation between critically stressed faults and permeability in fractured rocks. Given a current in-situ stress field in Holmedal with the maximum horizontal compressive stress oriented E–W to ESE–WNW, structures oriented in the ENE–WSW to SE–NW azimuthal sector would have the highest likelihood for reactivation, either by opening due to fracture-parallel compressive stresses or by induced shear stresses. This is consistent with the flow directions inferred from the pumping test.

Taken together, the pumping tests and the borehole geophysical information are consistent with a preferred groundwater flow in the ENE–WSW to SE–NW azimuthal sector, which contains the supposed direction of the largest horizontal stress in the area. Judged by the available draw-down and recovery data, N–S groundwater flow, at right angles to the predicted direction of the largest horizontal stress, is of less importance.

Testing of hypothesis (ii): Boreholes through major fracture lineaments

Five 13.8-cm diameter, open-bedrock wells were drilled by the down-the-hole hammer method (Driscoll 1986), targeting 2nd and 3rd order N–S lineaments of 7–15 km lengths at Folvåg, Herstad, Tysse and Vadheim (Fig. 2). At Herstad, a major E–W regional lineament (Standal Fault) runs ca. 300 m south of the well site. The bedrock types at the well sites are banded granitic gneisses (Herstad, Tysse and Vadheim) and meta-arkosic rocks (Folvåg).

The targeted lineaments are vertical or subvertical with narrow central parts (0–2 m), and the width of their proximal zones does not exceed 20 m. Each well was placed in the distal zone just outside the proximal zone of each lineament, and wells were drilled at right angles towards the lineament plunging at an angle of 60° . The total drilled length of each well was 100 m, corresponding to a vertical depth of ca. 86 m at the termination of the drillhole. With this design, the distal, proximal and central zones on both sides of the lineament would be intersected by the well, and

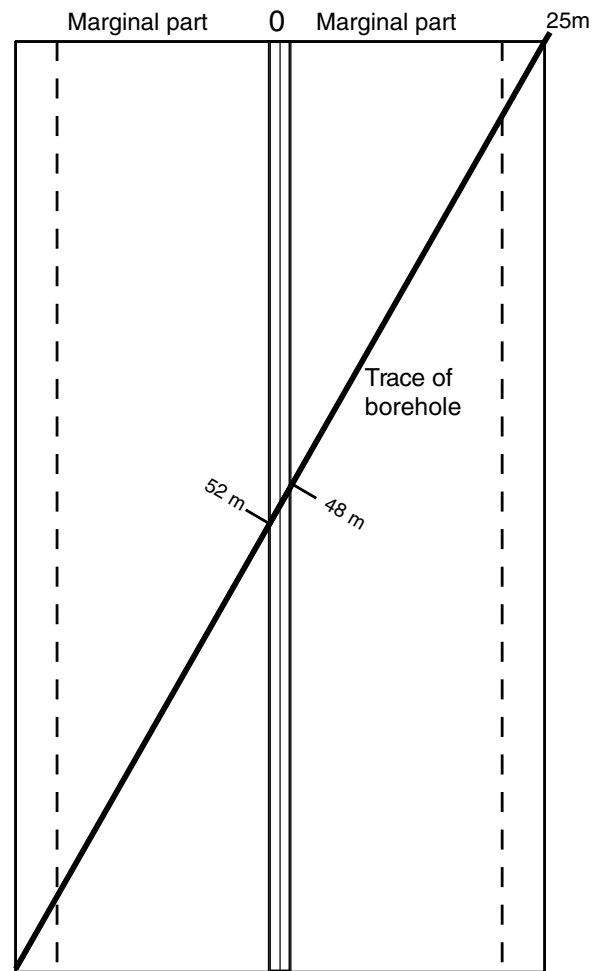


Fig. 7 Well design for wells targeted on N–S lineaments

the theoretically predicted central part of a vertical lineament is suspected to occur between 48 and 52 m along the section of the borehole (Fig. 7). However, due to deviations of borehole angles and lineament dips the depth to the actual intersection interval may vary slightly between wells. Descriptive logs with information about relative drill bit penetration rates, cuttings and water inflows were obtained during drilling. At the termination of the drilling, the capacity of each well was tested by air-lift methods. Some weeks later, short-term pumping tests were carried out in order to measure specific capacities listed in Table 3. Details of well design, methodology and pumping tests are found in Braathen et al. (1999) and Berg (2000). Later follow-up work with geophysical logging (OPTV, temperature, conductivity, natural gamma, resistivity, flow measurements) has been done on the well of Folvåg (Elvebakk et al. 2002).

Drillers log and pumping test data

Compilation of information from drilling logs may provide valuable information about rock type, fracture zones and transmissive fractures encountered along the section of the borehole (Cohen 1995; Paillet and Duncanson 1994).

Cuttings appear as finely ground particles in homogeneous rocks, whereas fractures and fracture zones produce larger and angular cuttings. When the drill bit meets a fracture, there is an increase in the rate of drill bit penetration. In larger fracture zones, the drill bit drops rapidly down until it meets more homogeneous rocks. Transmissive fractures can be identified as water is being transported to the surface together with the angular cuttings, and the water inflows at different depth intervals can thus be measured. Changes in rock types and mineralizations in otherwise homogeneous rocks will be revealed by colour changes in the cuttings. Fig. 8a shows a compilation of interpreted fracture zone locations and water inflows based on drillers logs for all five boreholes. In this figure, the wellbore is sectioned into intervals of one meter length, and the presence or absence of a fractured interval as interpreted from the driller's log is symbolized by black and white squares. In this manner, it is possible to carry out normal approximations of the single-sample runs tests (Sheskin 2000 p. 213) to evaluate whether the sequences of fractured and non-fractured intervals are distributed randomly, or form a discernible nonrandom pattern. The null hypothesis of this test is that the underlying population represented by the sequence of the two events has a random distribution.

For any of the five wellbore sections, the results support the alternative hypothesis of a nonrandom arrangement of the fractured and non-fractured sequences (Fig. 8b). The proximal part between 6–10 m from the central point of the lineament has the highest number of intersected fracture zones (8–9), but also the central part of the lineament has a high number (7) of fracture zones. Approximately 85% of the recorded fracture zones are within 18 m from the lineament centers, and all significant water inflows are also found in this part of the well sections which corresponds to the central and proximal zone of the lineaments (Fig. 8c).

Small-scale single-well pumping tests of about 6–12 h duration were performed as all wells were pumped at a constant pumping rate until approximate stable drawdowns were reached. After 1 h pumping was terminated, and the natural recovery of the water level was monitored until the original water level again was reached. Pumping test data are summarized in Table 3.

The recovery curves (Fig. 9) are directly related to the natural recharge to the well, and the inspection of these curves may provide information about the location and distribution of water transmissive fractures intersecting the

borehole. The recovery curve from Folvåg, starting at 32 m at 14:40, shows an exponential rise indicating a uniform fractured rock hydraulically similar to a porous aquifer. The curves for Tysse and Vadheim 1 have initially linear lower segments, starting at 73.5 m at 14:15 and 35 m at 12:00 respectively, followed by exponential rise at later stages indicating water entries from fractures evenly distributed along the borehole. The curves for Vadheim 2 and Herstad have linear trends, indicating that water entry is mainly from near surface fractures (Braathen et al. 1999).

Geophysical logging

Geophysical logs as a function of borehole length were obtained from the well in Folvåg and are shown in Fig. 10. The OPTV log identifies a highly fractured interval between 45 and 80 m, which is interpreted to represent the central and proximal zones of the lineament. Within this highly fractured interval the electrical resistivity curves display a marked decrease between 52 and 68 m, with a minimum at 58 m. Taking into account the actual borehole deviation, the predicted central zone of the lineament would be intersected in this interval. Accordingly, the resistivity anomaly is ascribed to the presence of conductive clay minerals in fault rocks present in the core of the lineament.

On either side of the central zone, the OPTV log shows ca. 15 m wide zones with high frequency of open fractures. The flowmeter, conductivity and temperature logs indicate water inflow at 46–47 m which correlates with the largest water strike ($3,600 \text{ l h}^{-1}$) recorded in the driller's log. In the flowmeter logs, changes in the net rotation speed (RPM) correlate with water inflows. Judged by the flowmeter logs (Elvebakk et al. 2002) the zone between 45 and 80 m, excluding the central core (54–60 m), alone stands for 70% of the water entry to the well and represents the inner proximal zone with enhanced fracture permeability. Minor water strikes are indicated in the outer proximal zone at 34 and 88 m.

In Fig. 11, box-plot comparisons between the well capacities for the 5 test wells drilled in the proximal zone of the lineaments and the 9 wells in Holmedal which occupy the distal/background zone are shown. Although the data set is small, the box-plot clearly indicates the higher groundwater potential for the proximal zone of the lineaments compared with the distal/background zone.

Table 3 Summary of well data for wells targeted on N–S lineaments

Well location	Depth (m)	Well yield at stable drawdown (l h^{-1})	Specific capacity ($\text{l h}^{-1} \text{ m}^{-1}$)	Well capacity from recovery tests (l h^{-1})
Folvåg	100	4,400	220	2,610
Tysse	100	142	2.3	1,840 ^a
Vadheim 1	102	No data	No data	13
Vadheim 2	100	400	22	1,320 ^a
Naustdal	100	692	13	612

^aCalculation based on inflow from lower section of well only

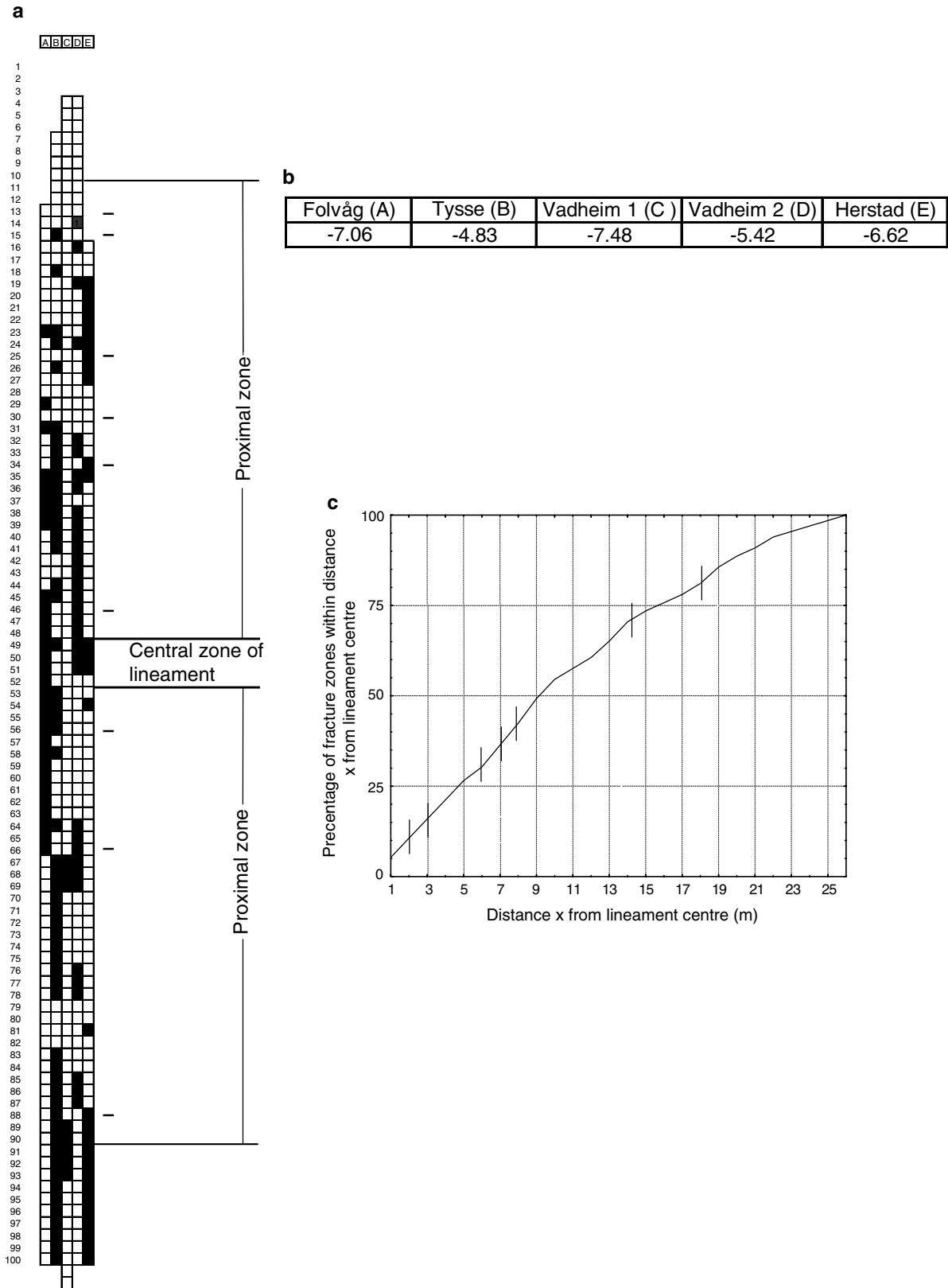


Fig. 8 a Occurrences of sequences with fractured and non-fractured intervals based on drillers logs for the five test boreholes. A fractured interval is symbolized with a *black square*, a non-fractured interval has no fill. The column to the left is the borehole length (m). A: Folvåg, B: Tysse, C: Vadheim 1, D: Vadheim 2, E: Herstad. Main

water strikes are indicated with *horizontal black lines*; **b** Table with *z-values* obtained during the single-sample runs tests; **c** Cumulative plot of fracture-zone frequency data in Fig. 8a. Main water strikes are indicated with *vertical black lines*

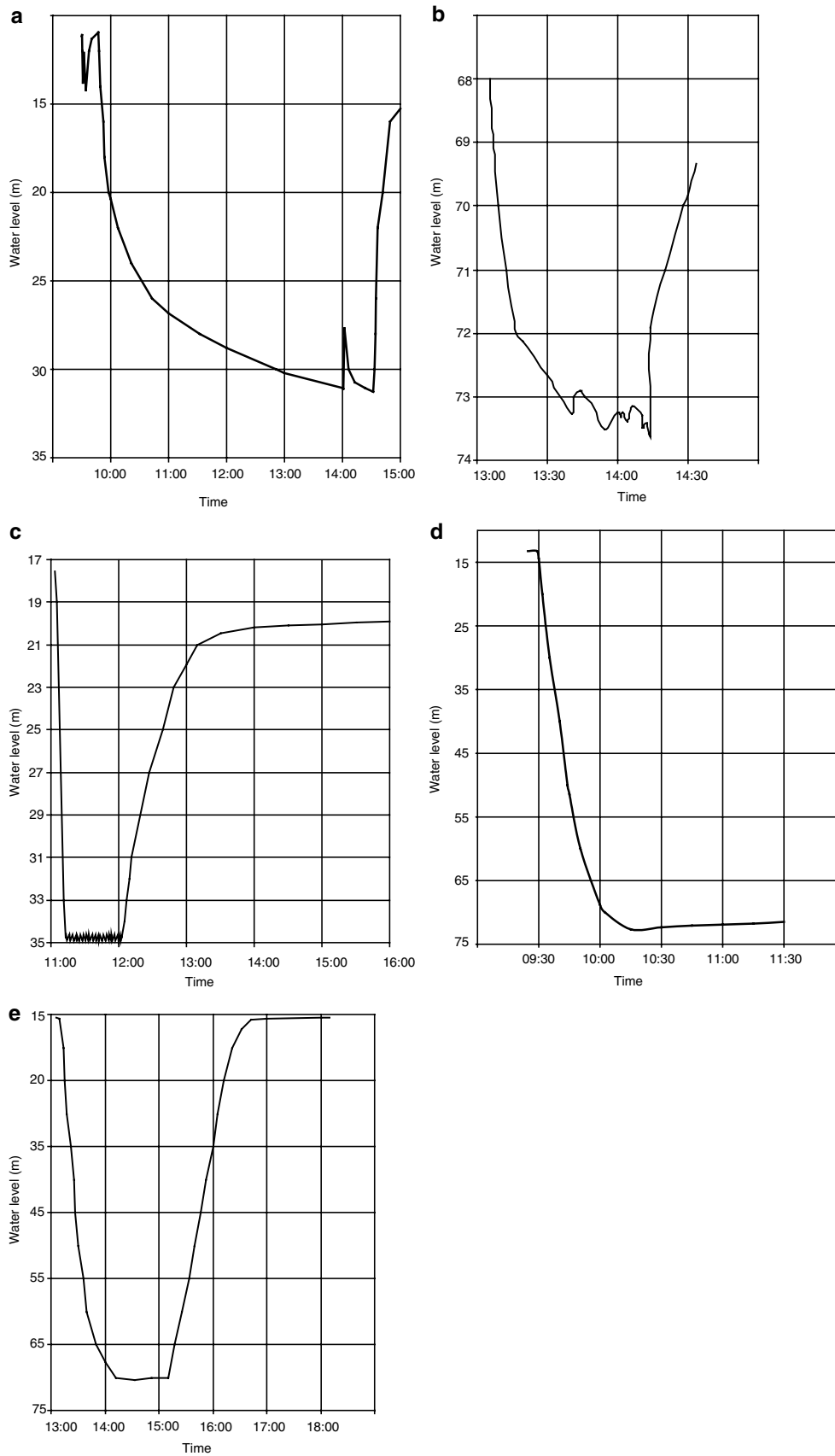
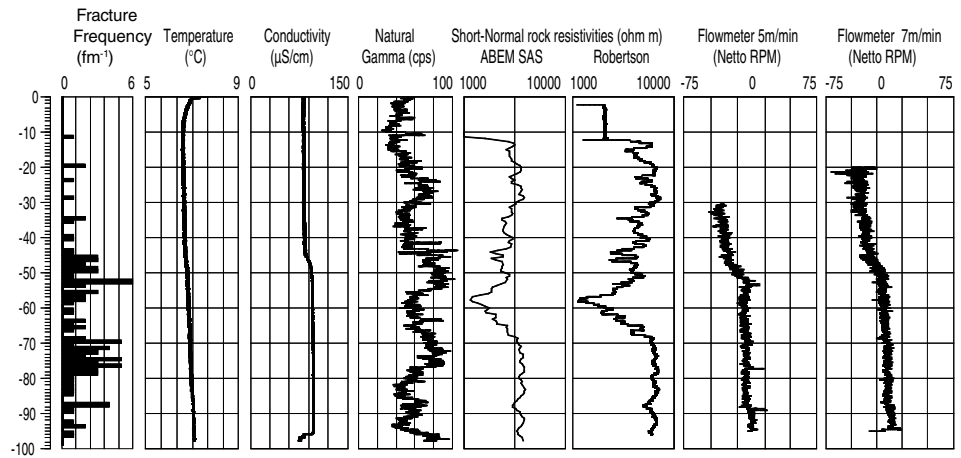


Fig. 9 Plots of drawdown and recovery data from the five test boreholes through the lineaments: **a** Folvåg; **b** Tysse; **c** Vadheim 1; **d** Vadheim 2 and **e** Herstad

Fig. 10 Geophysical logs for the Folvåg well, prepared from geophysical data by Elvebakk et al. (2002). The unit for fracture frequency is fractures per meter (fm^{-1})



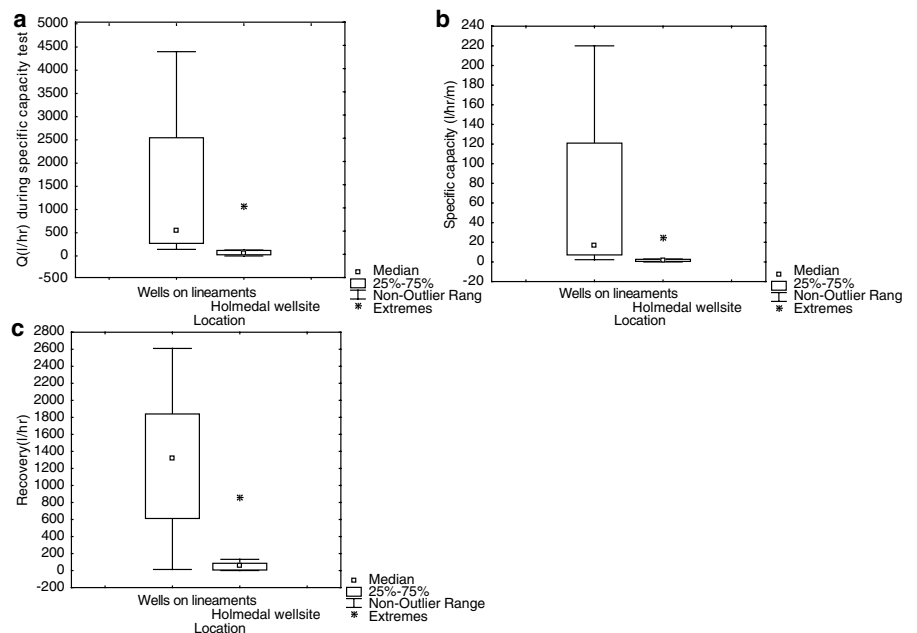
Discussion and conclusions

A phenomenon in nature, as the flow of groundwater in fractured crystalline hard rocks, is complex and is hardly understood by performing a single critical experiment with the aim to prove or disprove a scientific hypothesis. This is also the case in our work. The testing of the two hypotheses (i) In areas with a general background fracturing and in the distal zone of lineaments, groundwater flow will mainly occur along fractures parallel with the largest in-situ rock stress, and (ii) in the influence area of lineaments, the largest potential for groundwater abstraction is in the proximal zone - gives not a clear and unequivocal answer in support of the two assumptions about groundwater flow in the study area. However, most of the observed data are in agreement with the predictions from the models.

Since the Tertiary, high tectonic horizontal compressive stresses associated with ridge push from the mid-Atlantic ridge have been imposed on the western Fennoscandian

crust (Fejerskov et al. 2000). In combination with compressive stresses associated with postglacial doming (e.g. Gudmundsson 1999) and topographic effects, this produces high horizontal compressive stresses on the rock mass and existing fracture networks. Offshore stress data from borehole breakout measurements and fault plane solutions (Fejerskov et al. 2000; Lindholm et al. 2000; Dehls et al. 2000) as well as the onshore hydraulic fracturing data (Hansen 1996) are consistent with a regional compressive stress field in the outer Sunnfjord area with a main σ_H oriented E–W to ESE–WNW. Although the common magnitudes of σ_H are 10–20 MPa, horizontal compressive stresses exceeding 30 MPa have been recorded. In such a stress field, E–W-oriented fractures would have the lowest normal stress across them and tend to be pressed open, contrary to N–S fractures with a high angle to σ_H . The high compressive stresses recorded could also be capable of reactivating suitably oriented older faults and fractures by inducing shear stresses along these structures. Within such a current stress

Fig. 11 Box plot comparisons between well capacities for the five wells drilled through N–S fracture lineaments and the nine test wells in the Holmedal area located in the distal/background area with respect to a N–S fracture lineament: **a** Q (lh^{-1}) during specific capacity tests; **b** specific capacity ($\text{lh}^{-1} \text{m}^{-1}$) and **c** Q (lh^{-1}) from recovery test



field, structures at an approximate angle of 30° to σ_H would have the most favourable orientation for reactivation by slippage induced by shear stresses (Morris et al. 1996), and such critically stressed rocks would also be the most likely pathways for water flow through the fracture network (e.g. Barton et al. 1995; Ferril et al. 1999; Rogers 2003).

Given the orientation of the stress field in outer Sunnfjord, faults and fractures in the ENE–WSW to SE–NW azimuthal sector would have the greatest potential for reactivation. This prediction is supported by field evidence which show the invariable presence of younger and non-cohesive fault rocks of varying textures along the otherwise lithified cataclastic rocks along E–W faults (Andersen et al. 1999; Braathen et al. 1999). Many of the non-cohesive fault rocks are water conducting (Braathen et al. 1999). In the Holmedal well site, pumping tests and the geophysical logging information indicate that groundwater flow is mainly taking place along E–W to SE–NW fractures. These results are taken to reflect the effect of the in-situ present stress field acting on favourably oriented pre-existing fractures, favouring groundwater flow in the ENE–WSW to SE–NW azimuthal sector.

In light of the results from the Holmedal wellfield, it is therefore suggested that the current in-situ stress field exerts an important control on groundwater flow in the area studied, which is manifested by a preferred groundwater flow on faults and fractures in the ENE–WSW to SE–NW azimuthal sector outside the main influence areas of the multifracted N–S lineaments.

The results from the study of the N–S lineaments show that the hydromechanical properties of the fracture network favours groundwater flow in the proximal zone. The distal part and also areas outside the influence of lineaments have lower fracture frequencies and hence reduced fracture connectivity compared with the proximal part. The results from this work are also in agreement with the results of Evans et al. (1997).

Model (ii) is also verified by the pumping tests and geophysical logs from the test wells. The well capacities for the five wells drilled in the proximal zone of the lineaments are considerably higher than the well capacities for the nine wells in Holmedal which occupy the distal/background zone. However, in addition to the favourable hydromechanical structure of the proximal zone of the lineaments, others factors are probably also contributing to the higher groundwater potential of these structures. The lineaments coincide with valley bottoms or draws with generally thicker superficial cover, which make geomorphological influence and recharge conditions additional factors which explain the higher groundwater potential associated with the lineaments.

In conclusion, it is proposed that in this investigated setting of fractured hard rock, groundwater flow outside the influence area of lineaments is controlled by the action of the in-situ stress field on favourably oriented fractures, consistent with hypothesis (i).

The inner, proximal zone of multifracted lineaments represents an enhanced zone of fluid flow compared with the surroundings in accordance with hypothesis (ii).

Acknowledgements The fieldwork for this research was funded by the Geological Survey of Norway (NGU), project 2685.00. Pumping tests were performed by Gaute Storrø and Øystein Jæger, and geophysical measurements by Harald Elvebakk, Jan S. Rønning and Torleif Lauritsen, all employed at NGU. Silje Berg worked intensively with the five, hypothesis ii wells during her MSc work. One of the authors, Alvar Braathen, was employed at NGU while the project was running. We thank the Hydrogeology Journal reviewers for constructive and useful comments on the manuscript.

References

- Andersen TB, Jamtveit B (1990) Uplift of deep crust during orogenic extensional collapse: Model based on field studies in the Sogn-Sunnfjord region of W. Norway. *Tectonics* 9:1097–1111
- Andersen TB (1998) Extensional tectonics in the Caledonides of southern Norway, an overview. *Tectonophysics* 285:333–351
- Andersen TB, Torsvik TH, Eide EA, Osmundsen PT, Faleide JI (1999) Permian and Mesozoic extensional faulting within the Caledonides of central south Norway. *J Geol Soc Lond* 156:1073–1080
- Banks D, Odling NE, Skarphagen H, Rohr-Torp E (1996) Permeability and stress in crystalline rocks. *Terra Nova* 8:223–235
- Banks D (1991) Boring og prøvepumping av hydrogeologiske testhull i en grønnstein akvifer, Østmarkneset, Trondheim. (Drilling and test pumping of boreholes in a greenstone aquifer, Østmarkneset, Trondheim). *Geol Surv Norway Rep* 91.213
- Barton AB, Zoback MD, Moos D (1995) Fluid flow along potentially active faults in crystalline rock. *Geology* 23:683–686
- Berg SS (2000) Strukturell analyse av bruddsoner med hensyn på grunnvannspotensialet i oppsprukne bergarter. (Structural analysis of fracture zones in relation to groundwater potential in fractured rocks). MSc thesis, Department of Geology University of Bergen, (Norway)
- Braathen A, Henriksen H (1997) Post-Devonian fracture systems in the Sunnfjord region, onshore Western Norway. *Geol Surv Norway Bull* 433:16–18
- Braathen A (1999) Kinematics of post-Caledonian polyphase brittle faulting in the Sunnfjord region, western Norway. *Tectonophysics* 302:99–121
- Braathen A, Gabrielsen R (1998) Lineament architecture and fracture distribution in metamorphic and sedimentary rocks, with application to Norway. *Geol Surv Norway Rep* 98.043
- Braathen A, Gaut S, Henriksen H, Storrø G, Jæger Ø (1998) Holmedal brønnfelt, Sunnfjord: Geologiske undersøkelser og prøvepumping. (Holmedal well site, Sunnfjord: Geological investigations and test pumping). *Geol Surv Norway Rep* 98.085
- Braathen A, Berg S, Storrø G, Jæger Ø, Henriksen H, Gabrielsen G (1999) Bruddsonegeometri og grunnvannstrøm; resultater fra bruddstudier og testboringer i Sunnfjord. (Fracture-zone geometry and groundwater flow; results from fracture studies and test-drilling in Sunnfjord). *Geol Surv Norway Rep* 99.017
- Braathen A, Osmundsen PT, Gabrielsen RH (2004) Dynamic development of fault rocks in a crustal-scale detachment; an example from western Norway. *Tectonics* 23(4):TC4010, 27p
- Brook GA (1988) Hydrogeological factors influencing well productivity in the crystalline rocks of Georgia. *Southeastern Geol* 29:65–81
- Caine JS, Evans JP, Forster CB (1996) Fault zone architecture and permeability structure. *Geology* 24:1025–1028
- Chapman CA (1958) Control of jointing by topography. *J Geol* 66:552–558
- Cohen AJB (1995) Hydrogeologic Characterization of Fractured Rock Formations: A Guide for Groundwater Remediation Report LBL-38142, Earth Sciences Division Ernest Orlando Lawrence Berkeley National Laboratory Berkeley Lab. University of California, Berkeley, USA
- Dehls JF, Olesen O, Bungum H, Hicks EC, Lindholm CD, Riis F (2000) Neotectonic map: Norway and adjacent areas, 1:3,000,000. *Geol Surv Norway*

- Driscoll FG (1986) *Groundwater and Wells*. St. Paul. Johnson Division
- Eide EA, Torsvik TH, Andersen TB (1997) Absolute dating of brittle fault movements: Late Permian and Late Jurassic extensional fault breccias in western Norway. *Terra Nova* 9:135–139
- Eide EA, Torsvik TH, Andersen TB, Arnaud NO (1999) Early Carboniferous unroofing in western Norway: a tale of alkali feldspar thermochronology. *J Geol* 107:353–374
- Elvebakk H, Lauritsen T (1997) Geofysiske undersøkelser. Bruddsoner og grunnvann i Sunnfjord. (Geophysical investigations. Fracture zones and groundwater in Sunnfjord). *Geol Surv Norway Rep* 97.050
- Elvebakk H, Rønning JS (2002) Borehullslogging i fjellbrønn, Holmedal, Sunnfjord. Verifisering av hydrogeologisk model med hensyn til bergspenning, oppsprekking og strømningsretning. (Well logging of hard rock well, Holmedal, Sunnfjord. Verification of hydrogeological model with respect to rock stresses, fracturing and groundwater flow). *Geol Surv Norway Rep* 2002.093
- Elvebakk H, Rønning JS, Storrø G (2002) Borehullslogging i fjellbrønn, Follvåg, Sunnfjord. En verifisering av lineamentsmodel med hensyn til oppsprekking og vanngiverevne. (Well logging of hard rock well, Follvåg, Sunnfjord. A verification of lineament model with respect to fracturing and well yield). *Geol Surv Norway Rep* 2002.078
- Evans JP, Forster CB, Goddard JV (1997) Permeability of fault-related rocks and implications for hydraulic structure of fault zones. *J Struct Geol* 19:(11):1393–1404
- Fejerskov M, Lindholm CD (2000) Crustal stresses in and around Norway; an evaluation of stress generating mechanisms In: Nottvedt A (ed) *Dynamics of the Norwegian Margin*. *Geol Soc Lond Spec Publ No.* 167, pp 451–467
- Fejerskov M, Lindholm CD, Myrvang A, Bungum H (2000) Crustal stresses in and around Norway: a compilation of in situ stress observations. In: Nottvedt A (ed) *Dynamics of the Norwegian Margin*. *Geol Soc Lond Spec Publ No.* 167, pp 441–449
- Ferril DA, Winterle J, Wittmeyer G, Sims D, Colton S, Armstrong A (1999) Stressed rock strains groundwater at Yucca Mountain, Nevada *GSA Today* 9(5):1–8
- Gabrielsen R, Braathen A, Dehls J, Roberts D (2002) Tectonic lineaments of Norway. *Norwegian J Geol* 82:153–174
- Gaut S, Storrø G, Bjørnstad H, Braathen A (1999) Holmedal brønnfelt, Sunnfjord: Langtids prøvepumping og tracerester. (Holmedal well site, Sunnfjord: Long-term pumping tests and tracer experiments). *Geol Surv Norway Rep* 99.016
- Gernand JD, Heidtman JP (1997) Detailed pumping test to characterize a fractured bedrock aquifer. *Ground Water* 35(4):632–637
- Goldstein A, Marshak S (1988) Analysis of fracture array geometry. In: Marshak S, Mitra G (ed) *Basic methods of structural geology*. Prentice Hall. Englewood cliffs, New Jersey, 249–267
- Gudmundsson A (1999) Postglacial crustal doming, stresses and fracture formation with application to Norway. *Tectonophysics* 307:407–419
- Hancock PL (1985) Brittle Microtectonics: principles and practice. *J Struct Geol* 7(3/4):437–457
- Hansen SE (1996) Spenningsmåling ved hydraulisk splitting, Hestad og Atløy i Sogn og Fjordane. (Measurements of rock stresses by hydraulic splitting, Hestad and Atløy, Sogn og Fjordane). SINTEF Civil and Environmental Engineering Report STF22 F96090. Trondheim (Norway)
- Henning H, Elvebakk H (2001) Processing and analysis of acoustic borehole data from the Sunnfjord area and the Oslo region for evaluation of fracturing and possible water movements in rock). *Geol Surv Norway Intern Rep* 2001.14
- Henriksen H (1995) Relation between topography and borehole yield in boreholes in crystalline rocks, Sogn og Fjordane, Norway. *Ground Water* 33(4):635–643
- Henriksen H (2003) The role of some regional factors in the assessment of well yields from hard-rock aquifers of Fennoscandia. *Hydrogeol J* 11(6):628–645
- Kim G-B, Lee J-Y, Lee K-K (2004) Construction of lineament maps related to groundwater occurrence with Arcview and Avenue scripts. *Comp Geosci* 30(9/10):1117–1126
- Krásný J (2002) Quantitative hardrock hydrogeology in a regional scale. *Geol Surv Norway Bull* 439:7–14
- Lindholm CD, Bungum H, Hicks EC, Villagran M (2000) Crustal stress and tectonics in Norwegian regions determined from earthquake focal mechanisms. In: Nottvedt A (ed) *Dynamics of the Norwegian Margin*. *Geol Soc Lond Spec Publ No.* 167, pp 441–449
- Mabee SB (1998) Factors influencing well productivity in glaciated metamorphic rocks. *Ground Water* 37(1):88–97
- Midtbø E (1996) Bergspenninger på Nordvestlandet. (Rock Stresses in northwestern Norway). Project report NTNU, Institute for Geology and Rock Mechanics, Trondheim (Norway)
- Miller DJ, Dunne T (1996) Topographic perturbations of regional stresses and consequent fracturing. *J Geophys Res* 101:25523–25536
- Morin H, Savage WZ (2002) Topographic stress perturbations in southern Davis Mountains, west Texas 2. Hydrogeologic implications. *J Geophys Res* 107:(B122340), doi:10.1029/2001JB0004882002
- Morland G (1997) Petrology, Lithology, Bedrock Structures, Glaciation and Sea Level. Important Factors for Groundwater Yield and Composition of Norwegian Bedrock Boreholes? *Geol Surv Norway Rep* 97.122 I
- Morris AP, Ferril DA, Henderson DB (1996) Slip-tendency analysis and fault reactivation. *Geology* 24:275–278
- Nilsen B, Palstrøm A (2000) Engineering geology and rock engineering. Norwegian Group for Rock Mechanics, Oslo
- Norton MG (1987) The Nordfjord-Sogn Detachment, W. Norway. *Norsk Geol Tidsskrift* 67:93–106
- NRC (1996) Rock fractures and fluid flow. Contemporary understanding and applications. US National Research Council. National Academy Press, Washington, DC
- Osmundsen PT, Andersen TB (1994) Caledonian compressional and late-orogenic extensional deformation in the Staveneset area, Sunnfjord, Western Norway. *J Struct Geol* 16:1385–1401
- Osmundsen PT, Andersen TB (2001) The middle Devonian basins of western Norway: sedimentary response to large-scale transtensional tectonics? *Tectonophysics* 333:51–68
- Paillet F, Duncanson R (1994) Comparison of drilling reports and detailed geophysical analysis of ground-water production in bedrock wells. *Ground Water* 32(2):200–206
- Ramberg IB, Gabrielsen RH, Larsen BT, Solli A (1977) Analysis of fracture pattern in southern Norway. *Geol Mijnbouw* 56:295–310
- Rogers SF (2003) Critical stress-related permeability in fractured rocks. In: Ameen MS (ed) *Fracture and in-situ stress characterization of hydrocarbon reservoirs*. *Geol Soc Lond Spec Publ No.* 209, pp 7–16
- Rohr-Torp E (1994) Present uplift rates and groundwater potential in Norwegian hard rocks. *Geol Surv Norway Bull* 426:47–52
- Savage WZ, Swolfs HS, Powers PS (1985) Gravitational stresses in long symmetric ridges and valleys. *Int J Rock Mech Min Sci Geomech Abstr* 22(5):291–302
- Sayers CM (1990) Stress-induced fluid flow anisotropy in fractured rock. *Transport Porous Media* 5:287–297
- Sheskin DJ (2000) Parametric and nonparametric statistical procedures. Chapman and Hall, Boca Raton, FL, USA
- Singhal BBS, Gupta RP (1999) Applied hydrogeology of fractured rocks. Kluwer Academic, Dordrecht
- Valle V, Færseth RB, Fossen H (2002) Devonian-Triassic brittle deformation based on dyke geometry and fault kinematics in the Sunnhordland region, SW Norway. *Norwegian J Geol* 82:3–17
- Wise DU, McCrory TA (1982) A new method of fracture analysis: azimuth versus traverse distance plots. *Geol Soc Am Bull* 93:889–897